Inorg. Chem. **2005**, *44*, 758–769

Forum

Resonance Raman Investigation of the Specific Sensing Mechanism of a Target Molecule by Gas Sensory Proteins

Takehiro Ohta and Teizo Kitagawa*

Okazaki Institute for Integrative Bioscience, National Institutes of Natural Sciences, Okazaki, Aichi 444-8787, Japan

Received September 30, 2004

Specific sensing of gas molecules such as CO, NO, and O_2 is a unique function of gas sensory hemoproteins, while hemoproteins carry out a wide variety of functions such as oxygen storage/transport, electron transfer, and catalysis as enzymes. It is important in gas sensory proteins that the heme domain not only recognizes its target molecule but also discriminates against other gases having similar molecular structures. Coordination of a target molecule to the heme is assumed to alter the protein conformation in the vicinity of heme, and the conformation change is propagated to the effector domain where substrate turnover, DNA binding, or interaction with a signal transduction protein is performed differently than the binding of other gases. To understand the appearance of such a specificity, we focus our attention on the ligand–protein interactions in the distal side of heme. In practice, the metal–ligand vibrations as well as internal modes of ligand and heme are measured with resonance Raman spectroscopy for wild-type and some mutant proteins with full-length or limited sensory regions. On the basis of such observations together with the knowledge currently available, we discuss the mechanism of specific sensing of a diatomic molecule in gas sensory proteins.

Introduction

Specific sensing of gas molecules such as CO, NO, and O_2 is a unique function of gas sensory proteins.[1−3] XO (X = C, N, and O) molecules are charge-neutral and aprotic, providing no handle for interaction with polar or charged groups of proteins. Nature solved this problem by harnessing an Fe(II)−protoporphyrin IX (Chart 1) to the sensor domain of most gas sensory proteins, which is an effective binder of XO molecules. Owing to the suitable energy levels of the ferrous iron d_π orbitals in its heme complex that match well with those of XO π* orbitals, π back-donation takes place to the XO molecule according to the surroundings after coordination of a lone pair of electrons to the d_{z^2} orbital of ferrous iron.[4] As a result of back-bonding, polar residues in the distal heme pocket can yield stabilization energy through

Chart 1

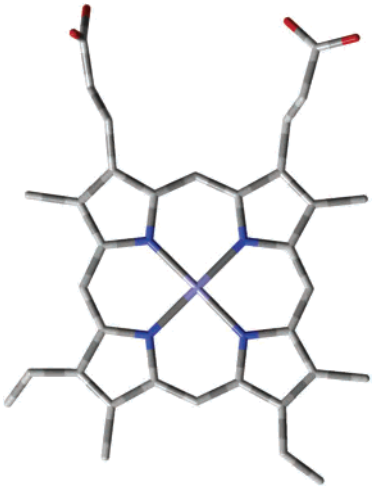

electrostatic interactions with the polarized heme-bound XO molecule in addition to specific hydrogen-bonding and van der Waals interactions.[4] The other concern of binding of the XO molecule to the transition metal center is that the binding

* To whom correspondence should be addressed. E-mail: teizo@ims.ac.jp.

(1) Rodgers, K. R. *Curr. Opin. Chem. Biol.* **1999**, *3*, 158−167.
(2) Chan, M. K. *Curr. Opin. Chem. Biol.* **2001**, *5*, 216−222.
(3) Jain, R.; Chan, M. K. *J. Biol. Inorg. Chem.* **2003**, *8*, 1−11.
(4) Spiro, T. G.; Jarzecki, A. A. *Curr. Opin. Chem. Biol.* **2001**, *5*, 715−723.

10.1021/ic0486318 CCC: $30.25
Published on Web 01/28/2005

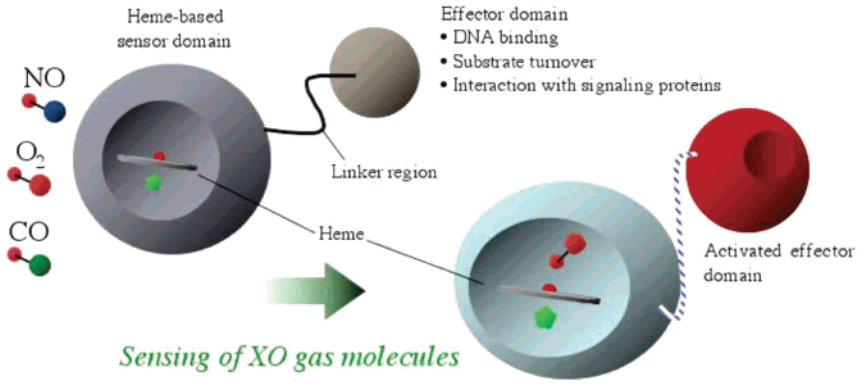

Figure 1. Functional scheme for gas sensory hemoproteins.

Table 1. Gas Sensory Hemoproteins

gas	sensors	functions	refs
CO	CooA	tanscriptional activator	26, 27
	NPAS2	transcriptional factor	28, 29
NO	sGC	guanylate cyclase	35−40
	HRI	phosphorylation of eIF2α for regulation of globin synthesis	41, 42
	(VCA0720)[a]	ND[b]	44
O_2	FixL	sensor kinase in FixL/FixJ two-component system	8−20
	DOS	phosphodiesterase	22−25
	AxPDEA1	phosphodiesterase, a regulator for cellulose syntesis	20
	HemAT	signal transducer for aerotaxis	30−34
	(Tar4)[a]	ND[b]	43−45

[a] Effector gas was tentatively assigned. [b] Not determined.

is accompanied with spin state alterations, which is formally a spin-forbidden reaction. Fortunately, heme groups have several excited states with unpaired electrons close in energy to the ground state[5−7] that can be used to enhance the probability of spin inversion, and this would be a quantum mechanical pathway to change the spin state of a molecule, despite the small spin−orbit coupling constant of the first transition metal.

Coordination of a target gas molecule to the heme-based sensor domain alters the protein conformation in the vicinity of the heme, and the structural change is propagated to the effector domain where substrate turnover, DNA binding, or interaction with a signal transduction protein is performed differently than the binding of other gases, as illustrated in Figure 1. The gas sensory proteins characterized to date are summarized in Table 1. For example, FixL includes a heme-PAS sensor domain (PAS is named as an arcronym for three sensor proteins PER, ARNT, and SIM) that activates genes required for bacterial nitrogen fixation by phosphorylating a partner protein, FixJ, and the phospho-FixJ subsequently binds to a regulation sequence of bacterial DNA.[8−20] FixL is inactivated when O_2 binds to its heme, and this is a mechanism that protects the nitrogen fixing proteins from oxidative damage. The *E. coli* direct oxygen sensor (*Ec*DOS), another member of a heme-PAS family,[21−25] is considered as an O_2 sensor or a redox sensor.[21,22] CooA, a CO sensor, controls the genes that code for proteins required for CO metabolism by bacteria.[26,27] CooA was the first example of a CO sensor protein, and its biochemical and biophysical aspects were extensively investigated during the past decade.[27] Neuronal PAS domain protein 2 (NPAS2), which is a mammalian transcriptional factor responsible for the regulation of circadian rhythm, is a heme-based CO sensor protein.[28,29] This is the first example of mammalian CO sensor proteins, and CO produced by the catabolism of heme by heme oxygenase (HO) is regarded as a neurotransmitter

(5) Harvery, J. N. *J. Am. Chem. Soc.* **2000**, *122*, 12401−12402.
(6) Franzen, S. *Proc. Natl. Acad. Sci. U.S.A.* **2002**, *99*, 16754−16759.
(7) Jensen, K. P.; Ryde, U. *J. Biol. Chem.* **2004**, *279*, 14561−14569.
(8) Gilles-Gonzalez, M. A.; Ditta, G. S.; Helinski, D. R. *Nature* **1991**, *350*, 170−172.
(9) Gilles-Gonzalez, M. A.; Gonzalez, G.; Perutz, M. F. *Biochemistry* **1995**, *34*, 232−236.
(10) Rodgers, K. R.; Lukat-Rodgers, G. S.; Barron, J. A. *Biochemistry* **1996**, *35*, 9539−9548.
(11) Lukat-Rodgers, G. S.; Rodgers, K. R. *Biochemistry* **1997**, *36*, 4178−4187.
(12) Gong, W.; Hao, B.; Mansy, S. S.; Gonzalez, G.; Gilles-Gonzalez, M. A.; Chan, M. K. *Proc. Natl. Acad. Sci. U.S.A.* **1998**, *95*, 15177−15182.
(13) Miyatake, H.; Mukai, M.; Adachi, S.; Nakamura, H.; Tamura, K.; Iizuka, T.; Shiro, Y.; Strage, R. W.; Hasnain, S. S. *J. Biol. Chem.* **1999**, *274*, 23176−23184.
(14) Rodgers, K. R.; Lukat-Rodgers, G. S.; Tang, L. *J. Am. Chem. Soc.* **1999**, *121*, 11241−11242.
(15) Rodgers, K. R.; Lukat-Rodgers, G. S.; Tang, L. *J. Biol. Inorg. Chem.* **2000**, *5*, 642−654.
(16) Gong, W.; Hao, B.; Chan, M. K. *Biochemistry* **2000**, *39*, 3955−3962.
(17) Miyatake, H.; Mukai, M.; Park, S.-Y.; Adachi, S.; Tamura, K.; Nakamura, H.; Nakamura, K.; Tsuchiya, T.; Iizuka, T.; Shiro, Y. *J. Mol. Biol.* **2000**, *301*, 415−431.
(18) Mukai, M.; Nakamura, K.; Nakamura, H.; Iizuka, T.; Shiro, Y. *Biochemistry* **2000**, *39*, 13810−13816.
(19) Hao, B.; Isaza, C.; Arndt, J.; Soltis, M.; Chan, M. K. *Biochemistry* **2002**, *41*, 12952−12958.
(20) Tomita, T.; Gonzalez, G.; Chang, A. L.; Ikeda-Saito, M.; Gilles-Gonzalez, M. A. *Biochemistry* **2002**, *41*, 4819−4826.
(21) Delgado-Nixon, V. M.; Gonzalez, G.; Gilles-Gonzalez, M. A. *Biochemistry* **2000**, *39*, 2685−2691.
(22) Sasakura, Y.; Hirata, S.; Sugiyama, S.; Suzuki, S.; Taguchi, S.; Watanabe, M.; Matsui, T.; Sagami, I.; Shimizu, T. *J. Biol. Chem.* **2002**, *277*, 23821−23827.
(23) Sato, A.; Sasakura, Y.; Sugiyama, S.; Sagami, I.; Shimizu, T.; Mizutani, Y.; Kitagawa, T. *J. Biol. Chem.* **2002**, *277*, 32650−32658.
(24) Gonzalez, G.; Dioum, E. M.; Bertolucci, C. M.; Tomita, T.; Ikeda-Saito, M.; Cheesman, M. R.; Watmough, N. J.; Gilles-Gonzalez, M. A. *Biochemistry* **2002**, *41*, 8414−8421.
(25) Park, H.; Suquet, C.; Satterlee, J. D.; Kang, C. *Biocheimstry* **2004**, *43*, 2738−2746.
(26) Shelver, D.; Kerby, R. L.; He, Y.; Roberts, G. P. *Proc. Natl. Acad. Sci. U.S.A.* **1997**, *94*, 11216−11220.
(27) Aono, S. *Acc. Chem. Res.* **2003**, *36*, 825−831.
(28) Dioum, E. M.; Rutter, J.; Tuckerman, J. R.; Gonzalez, G.; Gilles-Gonzalez, M.-A.; McKnight, S. L. *Science* **2002**, *298*, 2385−2387.
(29) Uchida, T.; Sato, E.; Sato, A.; Sagami, I.; Shimizu, T.; Kitagawa, T. *J. Biol. Chem.* To be published.

similarly to NO. The X-ray crystal structure of NPAS2 is not yet available, but a resonance Raman (RR) spectroscopic study was recently carried out to characterize the coordination environment of the heme, and its CO sensing mechanism was proposed.[29] HemAT is a myoglobin (Mb)-like O_2-sensing signal transducer protein responsible for aerotaxis control of bacteria,[30−33] and its detailed O_2-sensing mechanism[34] will be discussed in this article. Soluble guanylate cyclase (sGC), which is a signal transduction protein that responds to NO, catalyzes the formation of cyclic guanosine monophosphate (cGMP), an intracellular second messenger that interacts with an array of target proteins for vasodilation, neurotransmission, and inhibition of platelet aggregation.[35−40] A number of excellent reviews are available on many different aspects of sGC,[35,36] and recently, a review based on vibrational spectroscopic studies also became available.[39] Heme-regulated eukaryotic initiation factor 2α (eIF2α) kinase (HRI) regulates the synthesis of hemoglobin in reticulocytes in response to heme availability, and NO activates HRI catalysis by forming a five-coordinate heme−NO complex via Fe−His bond cleavage similarly to sGC.[41,42] sGC does not bind O_2, but one of the sGC-like heme domains from the *Thermoanaerobacter tengcongenesis* Tar4 protein (*Tt*Tar4), *Tt*Tar4H, is able to bind both NO and O_2, demonstrating ligand-binding properties similar to those of Mb.[43−45] This heme domain is specifically referred to as the heme−NO and $-O_2$ binding (H−NOX) domain.[43−45] Because *T. tengcongensis* is a strict anaerobe, it seems likely that *Tt*Tar4 serves as an O_2 sensor.[43,44]

The key issues in the study of heme-based gas sensory proteins are to elucidate how each of the crucial processes of sensing, including recognition, discrimination, and allostery, is achieved. For the cooperative oxygen binding of a paradigmatic allosteric hemoprotein, hemoglobin (Hb), a proximal allosteric pathway is emphasized,[46,47] because the strain on the Fe−His bond determines a low-O_2-affinity tense state (T state) and a high-O_2-affinity relaxed state (R state), as shown in Figure 2. However, if such a proximal pathway is the only way to convey the information of ligand binding, O_2 could not be distinguished from CO, because the two molecules form similar six-coordinate (6c) heme complexes in terms of the proximal geometry. Therefore, interaction of heme−XO adducts with proteins in the distal environment should play a crucial role in the sensing of gas molecules by gas sensory hemoproteins.

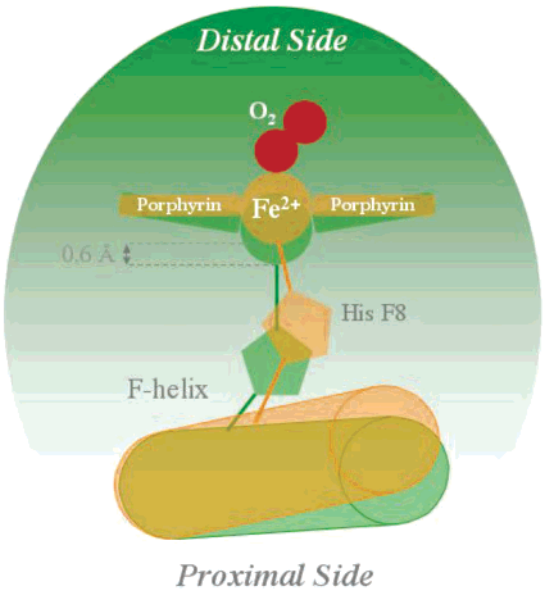

Figure 2. Mechanism of the T state (green) to R state (orange) transition in Hb.

Resonance Raman (RR) spectroscopy is a powerful tool for studying hemoproteins.[48] Assignments of several useful marker bands that are sensitive to the oxidation, coordination, and spin states of heme are known.[48,49] Furthermore, assignments of the heme−ligand vibrational modes have been established for several intrinsic and exogenous ligands.[50,51] Determination of the frequency of the iron−ligand stretching mode not only gives a direct estimate of the bond strength, but also allows conjectures as to how the surrounding environment interacts with heme−ligand adducts.

In this Forum article, we focus our attention on the ligand−protein interactions on the distal side of heme. In practice, the metal−ligand vibrations and internal modes of the ligand and heme are measured with RR spectroscopy for wild-type and some mutant proteins with full-length or limited sensory

(30) Hou, S.; Larsen, R. W.; Boudko, D.; Riley, C. W.; Karatan, E.; Zimmer, M.; Ordal, G. W.; Alam, M. *Nature* **2000**, *403*, 540−544.
(31) Hou, S.; Freitas, T.; Larsen, R. W.; Piatibratov, M.; Sivozhelezov, V.; Yamamoto, A.; Meleshkevitch, E. A.; Zimmer, M.; Ordal, G. W.; Alam, M. *Proc. Natl. Acad. Sci. U.S.A.* **2001**, *98*, 9353−9358.
(32) Aono, S.; Kato, T.; Matsuki, M.; Nakajima, H.; Ohta, T.; Uchida, T.; Kitagawa, T. *J. Biol. Chem.* **2002**, *277*, 13528−13538.
(33) Aono, S.; Nakajima, H.; Ohta, T.; Kitagawa, T. *Methods Enzymol.* **2004**, *381*, 618−628.
(34) Ohta, T.; Yoshimura, H.; Yoshioka, S.; Aono, S.; Kitagawa, T. *J. Am. Chem. Soc.* **2004**, *126*, 15000−15001.
(35) Wedel, B.; Humbert, P.; Harteneck, C.; Foerster, J.; Malkewitz, J.; Bohme, E.; Schultz, G.; Koesling, D. *Proc. Natl. Acad. Sci. U.S.A.* **1994**, *91*, 2592−2596.
(36) Ballou, D. P.; Zhao, Y.; Brandish, P. E.; Marletta, M. A. *Proc. Natl. Acad. Sci. U.S.A.* **2002**, *99*, 12097−12101.
(37) Makino, R.; Obayashi, E.; Homma, N.; Shiro, Y.; Hori, H. *J. Biol. Chem.* **2003**, *278*, 11130−11137.
(38) Pal, B.; Li, Z.; Ohta, T.; Takenaka, S.; Tsuyama, S.; Kitagawa, T. *J. Inorg. Biochem.* **2004**, *98*, 824−832.
(39) Pal, B.; Kitagawa T. *J. Inorg. Biochem.* **2005**, *99*, 267−279.
(40) Li, Z.; Pal, B.; Takenaka, S.; Tsuyama, S.; Kitagawa, T. *Biochemistry* **2005**, *44*, 939−946.
(41) Chen, J. J.; London, I. M. *Trends Biochem. Sci.* **1995**, *20*, 105−108.
(42) Igarashi, J.; Sato, A.; Kitagawa, T.; Yoshimura, T.; Yamauchi, S.; Sagami, I.; Shimizu, T. *J. Biol. Chem.* **2004**, *279*, 15752−15762.
(43) Gray, J. M.; Karow, D. S.; Lu, H.; Chang, A. J.; Chang, J. S.; Ellis, R. E.; Marletta, M. A.; Bargmann, C. I. *Nature* **2004**, *430*, 317−322.
(44) Karow, D. S.; Pan, D.; Tran, R.; Pellicena, P.; Presley, A.; Mathies, R. A.; Marletta, M. A. *Biochemistry* **2004**, *43*, 10203−10211.
(45) Pellicena, P.; Karow, D. S.; Boon, E. M.; Marletta, M. A.; Kuriyan, J. *Proc. Natl. Acad. Sci. U.S.A.* **2004**, *101*, 12854−12859.
(46) Perutz, M. F. *Nature* **1970**, *228*, 726−734.
(47) Voet, D.; Voet, J. G. *Biochemistry*; John Wiley & Sons: 1990.
(48) Spiro, T. G., Ed. *Biological Applications of Raman Spectroscopy*; Wiley: New York; 1988; Vol. III.
(49) Hu, S.; Smith, K. M.; Spiro, T. G. *J. Am. Chem. Soc.* **1996**, *118*, 12638−12646.
(50) Kitagawa, T. In *Biological Applications of Raman Spectroscopy*; Spiro, T. G., Ed.; Wiley-Interscience: New York, 1988; Vol. 3, pp 97−130.
(51) Yu, N.-T.; Kerr, E. A. In *Biological Applications of Raman Spectroscopy*; Spiro, T. G., Ed.; Wiley-Interscience: New York, 1988; Vol. 3, pp 39−95.

regions. On the basis of such observations together with the knowledge currently available, we discuss the mechanism of specific sensing of a diatomic molecule in gas sensory proteins.

RR Assignments of Heme−Ligand Vibrations

Our instrumental setup for RR spectroscopy can be found in ref 33. RR spectroscopy has a methodological characteristic of selective detection of vibrational modes of a certain chemical group whose electronic absorption band covers the Raman excitation wavelength, but infrared absorption spectroscopy does not involve such selective detection.[52,53] The vibrational modes of the active site of a hemoprotein and its associated ligands can be selectively enhanced by tuning the excitation wavelength to the absorption bands of the heme. The vibrational modes of protein backbones retain the much weaker Raman scattering and, in practice, are not detected above the spectral background unless Raman scattering is excited by an ultraviolet laser in resonance with absorption bands of amino acid residues. However, the effects of the protein structure on the heme and its coordinated ligands can be investigated by examining changes in the heme and heme−ligand vibrational modes resulting from modifications of the protein structure by site-directed mutagenesis. Next, we discuss the currently available knowledge of heme−ligand vibrations revealed by RR spectroscopy.

Heme−CO Adduct. CO binds to ferrous heme iron in a linear Fe−C−O geometry with very high affinity. In a protein matrix, however, Fe−C−O is slightly bent mainly because of electrostatic interactions from distal environments.[54,55] The heme−ligand interaction provided evidence that the heme pocket was most extensively investigated by heme−CO adducts, because heme−CO adducts are stable compared to heme−NO and $-O_2$ adducts and the vibrations involved in Fe−C−O are very sensitive to the polarity and steric effects from the distal environment.[55] Three normal vibrations associated with the Fe−C−O linkage, Fe−CO stretching (ν_{Fe-CO}), Fe−C−O bending (δ_{Fe-C-O}), and C−O stretching (ν_{C-O}), are detectable with Soret excitation for heme−CO adducts.[51] The stretching and bending vibrations can be assigned on the basis of sensitivity to CO isotopes; as the total mass increases (in the order $^{12}C^{16}O$, $^{13}C^{16}O$, $^{12}C^{18}O$, $^{13}C^{18}O$), the vibrational frequencies show a monotonic downshift for ν_{Fe-CO}, whereas the sensitivity zigzags for δ_{Fe-C-O}.[51] The ν_{Fe-CO} RR band appears in the spectral range of 470−550 cm^{-1}. The ligand internal vibration, ν_{C-O}, is detected in the 1800−2000 cm^{-1} region.

The ν_{Fe-CO} and ν_{C-O} frequencies are linearly correlated with a negative coefficient; as back-donation increases, the ν_{Fe-CO} and ν_{C-O} frequencies show an upshift and a downshift, respectively.[56] When the environment surrounding CO becomes positive, π-electrons are more delocalized from Fe to CO, and as a result, the C−O bond becomes weaker because of increased population in the CO antibonding orbital but the Fe−CO bond becomes stronger.[55] The delocalization of π-electrons is reflected in the ν_{C-O} and ν_{Fe-CO} frequencies. Thus, the ν_{Fe-CO} and ν_{C-O} frequencies are a good indicator of distal pocket polarity.[55] The δ_{Fe-C-O} RR band is observed in the range of 550−580 cm^{-1} and has a frequency that is sensitive to the ^{13}C isotope because of the larger vibrational displacement of the C atom. A higher frequency for bending than for stretching is unusual among chemical bonds. However, density functional theory (DFT) computations explain this peculiarity in terms of electrostatic and steric barriers from the surrounding protein residues.[54,57] It was previously proposed that the δ_{Fe-C-O} RR band in the range of 550−580 cm^{-1} was not the fundamental bending mode but rather its overtone or a combination band involving the bending mode and a porphyrin vibration.[58−60] The basic idea behind such a proposal is that δ_{Fe-CO} belongs to the E symmetry species within the framework of the idealized C_{4v} point group of a heme−CO adduct and lacks a mechanism for RR enhancement via either the Franck−Condon A term mechanism, which applies only to totally symmetric modes, or the vibronic B term mechanism, which applies to modes of A_2, B_1, and B_2 symmetry species to couple with the $\pi-\pi^*$ electronic transitions of heme.[53,61] Hirota et al. assigned the bending fundamental to a CO-isotope-sensitive band at 365 cm^{-1} in the RR spectra of CO-bound Hb and other hemoproteins.[59,60] The overtone proposal requires that the fundamental be present around 290 cm^{-1}, where no CO-isotope-sensitive band was found in IR spectra for model compounds.[58] However, the consensus might have been obtained for the δ_{Fe-C-O} RR band assignment at 550−580 cm^{-1} after FT-IR observation of the bending mode for model compounds.[62] The intensity ratio between the ν_{Fe-CO} and δ_{Fe-C-O} RR bands is considered as an indicator of the off-axis geometry of Fe−C−O or its dipole because of interaction from the distal side.[61]

Heme−NO Adduct. NO, having one electron more than CO, binds to ferrous heme iron in a bent geometry.[63] NO can also form an adduct with ferric heme iron yielding a linear geometry similar to that of ferrous CO heme, but its affinity ($K_d \approx 1 \times 10^{-4}$ M^{-1}) is much lower than that of ferrous hemes ($K_d \approx 1 \times 10^{-14}$ M^{-1}). In addition, the physiologically important iron oxidation state is the ferrous state in the NO sensor of sGC.[35−40] The three normal

(52) Wilson, E. B., Jr.; Decius, J. C.; Cross, P. C. *Molecular Vibrations—The Theory of Infrared and Raman Vibrational Spectra*; Dover Publications: New York, 1980.
(53) Czernuszewicz, R. S.; Spiro, T. G. In *Inorganic Electronic Structure And Spectroscopy*; Solomon, E. I., Lever, A. B. P., Eds.; Wiley-Interscience: New York, 1999; Vol. I, pp 353−441.
(54) Spiro, T. G.; Kozlowski, P. M. *Acc. Chem. Res.* **2001**, *34*, 137−144.
(55) Phillips, G. N., Jr.; Teodoro, M. L.; Li, T.; Smith, B.; Olson, J. S. *J. Phys. Chem. B* **1999**, *103*, 8817−8829.
(56) Vogel, K. M.; Kozlowski, P. M.; Zgierski, M. Z.; Spiro, T. G. *J. Am. Chem. Soc.* **1999**, *121*, 9915−9921.
(57) Ghosh, A.; Bocian, D. F. *J. Phys. Chem.* **1996**, *100*, 6363−6367.
(58) Tsuboi, M. *Indian J. Pure Appl. Phys.* **1988**, *26*, 188−191.
(59) Hirota, S.; Ogura, T.; Shinzawa-Itoh, K.; Yoshikawa, S.; Nagai, M.; Kitagawa, T. *J. Phys. Chem.* **1994**, *98*, 6652−6660.
(60) Hirota, S.; Ogura, T.; Kitagawa, T. *J. Am. Chem. Soc.* **1995**, *117*, 821−822.
(61) Ray, G. B.; Li, X.-Y.; Ibers, J. A.; Sessler, J. L.; Spiro, T. G. *J. Am. Chem. Soc.* **1994**, *116*, 162−176.
(62) Hu, S.; Vogel, K. M.; Spiro, T. G. *J. Am. Chem. Soc.* **1994**, *116*, 11187−11188.
(63) Hoffman, R.; Chen, M. M. L.; Thorn, D. L. *Inorg. Chem.* **1977**, *16*, 503−511.

vibrations associated with the ferrous Fe−N−O linkage, Fe−NO stretching (ν_{Fe-NO}), Fe−N−O bending (δ_{Fe-N-O}), and N−O stretching (ν_{N-O}), are detectable with Soret excitation for heme−NO adducts.[51] The ν_{Fe-NO} RR band appears in the spectral range of 520−530 cm^{-1} (5c heme−NO adducts) or 540−560 cm^{-1} (6c heme−NO adducts).[11] The ligand internal vibration, ν_{N-O}, is detected in the 1550−1700 cm^{-1} region.[11] The δ_{Fe-N-O} band is observed in the range of 400−500 cm^{-1},[11] which is sensitive to the ^{15}N isotope. The ν_{Fe-NO} and ν_{N-O} frequencies are negatively correlated, but the correlation is weak compared to the ν_{Fe-CO}/ν_{C-O} correlation.[64−66]

Recently, the nature of the distal residue interaction on heme-bound NO was analyzed systematically using a number of mutant Mb's by Spiro and co-workers.[66] They suggested that steric forces that alter the Fe−N−O geometry are responsible for the complex behavior of the ν_{Fe-NO}/ν_{N-O} correlation and provided substantial support for this view via a DFT calculation.[66] On the other hand, Boxer et al. pointed out that the weak ν_{Fe-NO}/ν_{N-O} correlation is due to the small electronic polarizability of the Fe−NO bond, possibly because of weak back-bonding in heme−NO adducts.[65] Thus, a consensus might have not been acquired regarding the heme−NO back-bonding mechanism. The peculiar nature of NO binding to heme is its negative trans effect,[67−69] a mechanism by which the trans axial ligand is detached from heme iron, forming a 5c heme−NO adduct. This effect is particularly notable for the ferrous state. It is worth noting that, when iron nitrosyl is in the ferric oxidation state, the ligand internal vibrational mode can be strongly enhanced by a 244-nm RR excitation.[70] This UV RR enhancement is not coupled with a charge transfer from a heme to the NO ligand, and its mechanism remains to be explored. A recent DFT work has also indicated unique aspects of the bonding in {FeNO}^{6} porphyrinates, suggesting that the bonding in FeNO complexes is indeed not as simple as that in FeCO complexes.[71]

Heme−O_2 Adduct. O_2 binds to a ferrous heme iron with the lowest affinity among XO molecules, and autoxidation occurs for the heme−O_2 adduct,[47] which makes a study of this species difficult. There are three normal vibrations associated with the Fe−O−O linkage, Fe−O_2 stretching (ν_{Fe-O_2}), Fe−O−O bending (δ_{Fe-O-O}), and O−O stretching (ν_{O-O}), which are, in principle, detectable upon Soret excitation for heme−O_2 adducts.[51] The ν_{Fe-O_2} frequency appears in the spectral range of 550−570 cm^{-1}. Indirect methods, such as replacing the heme iron by cobalt, were used to measure the ν_{O-O} frequency, because the ν_{O-O} RR band was hardly enhanced in iron porphyrin complexes.[72−77] There has been no consensus on the unperturbed ν_{O-O} frequency of oxyhemoglobin, because the mode displays substantial vibrational coupling with internal modes of the trans ligand,[74−77] resulting in a complex splitting pattern. Kincaid and co-workers pointed out that the complicated ν_{O-O} spectral pattern of cobalt porphyrin−imidazole complexes is due to vibrational coupling between ν_{O-O} and internal vibrations of the trans-coordinated imidazole ligand, based on strategic isotopic labeling experiments employing O_2 isotopes and selectively deuterated imidazole compounds.[75] It is quite important to find the unperturbed ν_{O-O} frequency from the observed spectrum in order to discuss electronic properties of bound O_2. It was recently demonstrated that, when heme-bound O_2 is strongly H-bonded from the distal side, the ν_{Fe-O_2} and ν_{O-O} RR bands can be simultaneously enhanced.[78] Limited examples are available for δ_{Fe-O-O} RR bands assigned in the range of 340−500 cm^{-1}.[79,80] Electrostatic interactions from distal environments seem to scarcely affect the nature of Fe−O_2 bonding in the case of Mb and its mutants,[81] which is distinct from the case of Fe−CO bonding.

Such fundamental understanding of Fe−X−O vibrations and bonding in the paradigmatic hemoprotein Mb as well as heme model compounds is crucial for elucidation of the interaction of proteins with heme-bound ligands, and the concepts developed in this area have been applied to the studies on sensing mechanisms of gas sensory proteins. In the subsequent sections, we discuss our own RR spectroscopic studies on an oxygen sensor protein, wild-type HemAT-*Bs* and its mutants obtained from site-directed mutagenesis, in which Fe−O_2 bonding is examined in detail. Analyses of the ν_{Fe-O_2} band provided a clue for understanding of the O_2 sensing mechanism of a HemAT-*Bs* protein.

General Properties of the O_2 Sensor HemAT-*Bs* Protein

HemAT-*Bs* is a heme-containing signal transducer protein responsible for aerotaxis of *Bacillus subtilis*.[30,31] Specific sensing of O_2, CO, and NO might have been required for the aerophilic bacteria in the early times on Earth, when CO and NO were more abundant than O_2.[82] In support of this

(64) Tomita, T.; Hirota, S.; Ogura, T.; Olson, J. S.; Kitagawa, T. *J. Phys. Chem. B* **1999**, *103*, 7044−7054.
(65) Park, E. S.; Boxer, S. G. *J. Phys. Chem. B* **2002**, *106*, 5800−5806.
(66) Coyle, C. M.; Vogel, K. M.; Rush, T. S. III, Kozlowski, P. M.; Williams, R.; Spiro, T. G.; Dou, Y.; Ikeda-Saito, M.; Olson, J. S.; Zgierski, M. Z. *Biochemistry* **2003**, *42*, 4896−4903.
(67) Schelvis, J. P. M.; Seibold, S. A.; Cerda, J. F.; Garavito, R. M.; Babcock, G. T. *J. Phys. Chem. B* **2000**, *104*, 10844−10850.
(68) Rovira, C.; Kunc, K.; Hutter, J.; Ballone, P.; Parrinello, M. *J. Phys. Chem. A* **1997**, *101*, 8914−8925.
(69) Marti, M. A.; Scherlis, D. A.; Doctorovich, F. A.; Ordejon, P.; Estrin, D. A. *J. Biol. Inorg. Chem.* **2003**, *8*, 595−600.
(70) Tomita, T.; Haruta, N.; Aki, M.; Kitagawa, T.; Ikeda-Saito, M. *J. Am. Chem. Soc.* **2001**, *123*, 2666−2667.
(71) Linder, D. P.; Rodgers, K. R.; Banister, J.; Wyllie, G. R. A.; Ellison, M. K.; Scheidt, W. R. *J. Am. Chem. Soc.* **2004**, *126*, 14136−14148.
(72) Tsubaki, M.; Yu, N. T. *Proc. Natl. Acad. Sci. U.S.A.* **1981**, *78*, 3581−3585.
(73) Kitagawa, T.; Ondrias, M. R.; Rousseau, D. L.; Ikeda-Saito, M.; Yonetani, T. *Nature* **1982**, *298*, 869−871.
(74) Bajdor, K.; Kincaid, J. R.; Nakamoto, K. *J. Am. Chem. Soc.* **1984**, *106*, 7741−7747.
(75) Bruha, A.; Kincaid, J. R. *J. Am. Chem. Soc.* **1988**, *110*, 6006−6014.
(76) Proniewicz, L. M.; Kincaid, J. R. *J. Am. Chem. Soc.* **1990**, *112*, 675−681.
(77) Proniewicz, L. M.; Kincaid, J. R. *Coord. Chem. Rev.* **1997**, *161*, 81−127.
(78) Das, T. K.; Couture, M.; Ouellet, Y.; Guertin, M.; Rousseau, D. L. *Proc. Natl. Acad. Sci. U.S.A.* **2001**, *98*, 479−484.
(79) Hirota, S.; Ogura, T.; Appelman, E. H.; Shinzawa-Itoh, K.; Yoshikawa, S.; Kitagawa, T. *J. Am. Chem. Soc.* **1994**, *116*, 10564−10570.
(80) Macdonald, I. D. G.; Sligar, S. G.; Christian, J. F.; Unno, M.; Champion, P. M. *J. Am. Chem. Soc.* **1999**, *121*, 376−380.
(81) Hirota, S.; Li, T.; Phillips, G. N., Jr.; Olson, J. S.; Mukai, M.; Kitagawa, T. *J. Am. Chem. Soc.* **1996**, *118*, 7845−7846.

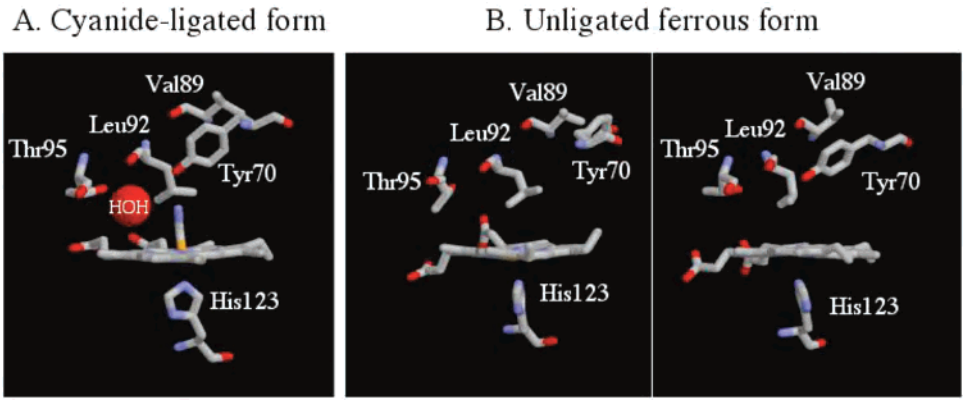

Figure 3. Structure of the sensor domain of HemAT-*Bs*. (A) X-ray crystal structure of cyanide ligated HemAT-*Bs* sensor domain (PDB code 1OR4). (B) Asymmetric dimer active site of ferrous unligated HemAT-*Bs* sensor domain (PDB code 1OR6).

idea, our RR study of the O_2-bound form of HemAT-*Bs* has demonstrated that the ν_{Fe-O_2} frequency (560 cm^{-1}) is noticeably lower than those of general O_2-bound hemoproteins[32] but similar to the frequencies observed for invertebrate, plant, and bacterial Hb's,[78,83] suggesting that the heme-bound O_2 is incorporated into a unique hydrogen-bonding network in the distal environment. However, the O_2 binding and dissociation rate constants were ordinary, revealing that HemAT-*Bs* has a moderate O_2 affinity similar to that of Mb.[32] Thus, the ligand discrimination mechanism as an O_2 sensor must employ a ligand-dependent allostery to overcome this disadvantage of high affinity for CO.

Phillips et al. recently determined the X-ray structures of the unligated and cyanide (CN)-ligated forms of the sensor domain of HemAT-*Bs* (Figure 3).[84] The sensor domain protein maintains a classic globin fold and forms a homodimer structure. The active site of the heme-based sensor domain of the CN-bound form (Figure 3A) contains a unique distal heme pocket surrounded by Tyr70, Thr95, and a water molecule. Because Tyr70 exhibits distinct conformational changes in one subunit, as shown in Figure 3B, when the ligands are removed, the symmetry breaking of HemAT-*Bs* was proposed to play an important role in initiating the chemotaxis signaling transduction cascade.[84]

Distal Sensing Mechanism of HemAT-*Bs* Protein

The X-ray structure of the unligated and CN-ligated truncated sensor domain protein indicated that Tyr70, Thr95, and a water molecule might play a crucial role in sensing mechanism of HemAT-*Bs*. Thus, we examined the protein−ligand interaction by RR spectroscopy in conjunction with site-directed mutagenesis studies. Figure 4 shows the observed RR spectra of O_2-bound HemAT-*Bs* and its mutants in the ν_{Fe-O_2} frequency region, together with the results from the band-fitting analyses.[34]

The band-fitting analyses located the centers of oxygen-isotope-sensitive Gaussian bands at 554, 566, and 572 cm^{-1} for the WT form as delineated by the red dotted lines in Figure 4A (a), which are shifted to 537, 547, and 554 cm^{-1}, respectively, with $^{18}O_2$, as shown in Figure 4A (b). The $^{16}O_2$-minus-$^{18}O_2$ difference spectrum yields a single peak and valley as depicted by Figure 4A (c). In D_2O, the oxygen-isotope-sensitive band(s) exhibited an upshift from 565 to 576 cm^{-1} as seen in the H_2O-minus-D_2O difference spectrum [Figure 4A (d)], indicating that a H-bond(s) is formed between the bound oxygen and a protein residue.[73] Thus, there would be multiple conformations of weakly and strongly H-bonded forms, which are tentatively called the open and closed forms. The closed form has the strongly H-bonded O_2 with ν_{Fe-O_2} at 554 cm^{-1}, whereas the open form has the weakly interacting O_2 with ν_{Fe-O_2} at 566 and 572 cm^{-1}. The open form would provide the moderate O_2 affinity (K_d = 719 nM, where $K_d = k_{off}/k_{on}$) for HemAT-*Bs*,[32] because the open form would release heme-bound O_2 easily.

Because a H-bond to the sp^2 orbital of the proximal O atom of heme-bound O_2 would weaken the Fe−O_2 bond as indicated by the low ν_{Fe-O_2} frequency, a water molecule found by X-ray analyses[84] that was H-bonded by Thr95 in the cyanide-ligated form would be involved in such a strong H-bonding interaction in the closed form. Because the position of this water molecule can be slightly displaced to keep the same D-bond strength, the 554 cm^{-1} band does not show a H_2O/D_2O frequency shift despite strong H-bonding. There is also an observation that a strongly H-bonded heme−O_2 adduct with a low ν_{Fe-O_2} frequency is deuterium-insensitive.[78] In support of this idea, the T95A mutant, in which the water molecule cannot be present in the hydrophobic environment, gave a single oxygen-isotope-sensitive band centered at 569 cm^{-1} as shown in Figure 4D (a). These results show that the O_2-bound T95A mutant has a single conformation of the distal heme pocket, yielding the open form with ν_{Fe-O_2} = 572 cm^{-1} for WT. For the T95A mutant, the interaction of Thr95 with the proximal O atom of heme-bound O_2 is absent, and therefore, the 554 cm^{-1} band disappears. In other words, Thr95 is essential for maintaining the closed form.

Whereas the ν_{Fe-O_2} bands were affected by the mutation of Thr95, the mutation of Tyr70 showed little effect on the ν_{Fe-O_2} bands. The ν_{Fe-O_2} bands of the Y70F mutant were fitted with three bands at 555, 566 and 573 cm^{-1} [Figure

(82) Kasting, J. F. *Science* **1993**, *259*, 920−926.
(83) Yeh, S.-R.; Couture, M.; Ouellet, Y.; Guertin, M.; Rousseau, D. L. *J. Biol. Chem.* **2000**, *275*, 1679−1684.
(84) Zhang, W.; Phillips, G. N., Jr. *Structure* **2003**, *11*, 1097−1110.

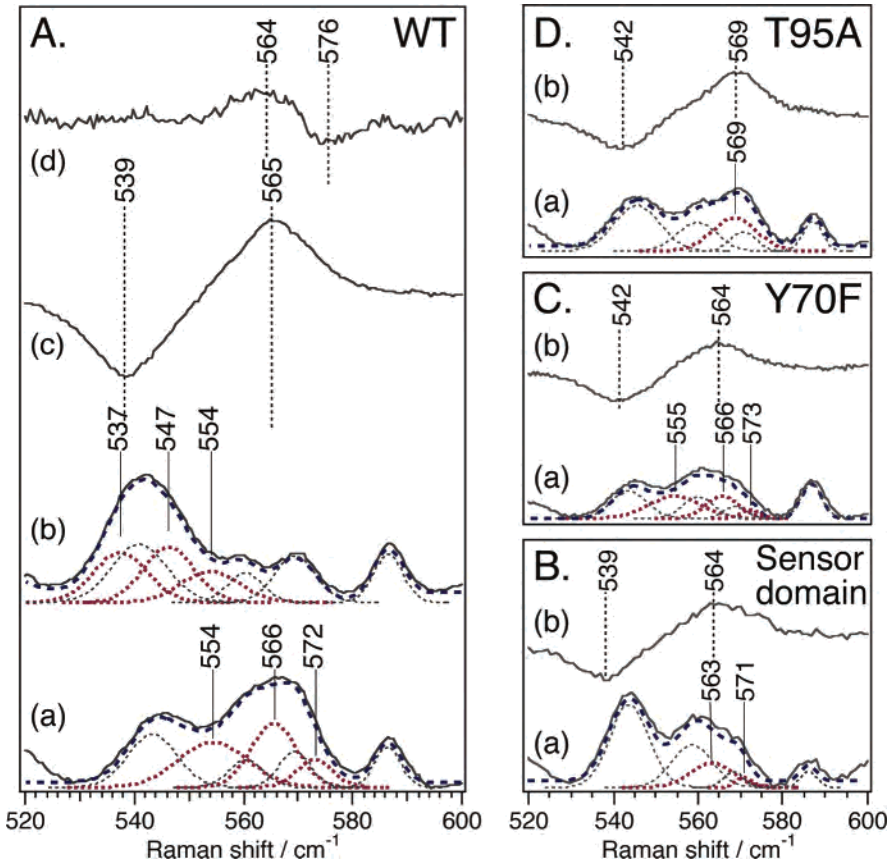

Figure 4. Resonance Raman spectra of O_2-bound WT and mutants HemAT-*Bs*. (A) (a) $^{16}O_2$- and (b) $^{18}O_2$-bound WT HemAT-*Bs* in H_2O, (c) $^{16}O_2 - {}^{18}O_2$ difference spectrum, and (d) difference spectrum between the $^{16}O_2$-bound forms in H_2O and D_2O ($H_2O - D_2O$). (B) (a) Spectrum of the $^{16}O_2$-bound truncated sensor domain in H_2O and (b) $^{16}O_2 - {}^{18}O_2$ difference spectrum. (C) (a) $^{16}O_2$-bound Y70F mutant HemAT-*Bs* in H_2O and (b) $^{16}O_2 - {}^{18}O_2$ difference spectrum . (D) (a) $^{16}O_2$-bound T95A mutant HemAT-*Bs* in H_2O and (b) $^{16}O_2 - {}^{18}O_2$ difference spectrum. In all traces a, the dashed and dotted lines were obtained by Gaussian band-fitting analyses. The dark red dotted lines denote the contributions from ν_{Fe-O_2}. The gray dotted lines show heme modes, and two of them overlapped with the ν_{Fe-O_2} bands were estimated from the spectra of the $^{18}O_2$-bound forms. The navy blue dashed lines are the sums of the component bands. All difference spectra are raw spectra without scaling. Reprinted with permission from ref 34. Copyright 2004 American Chemical Society.

Scheme 1

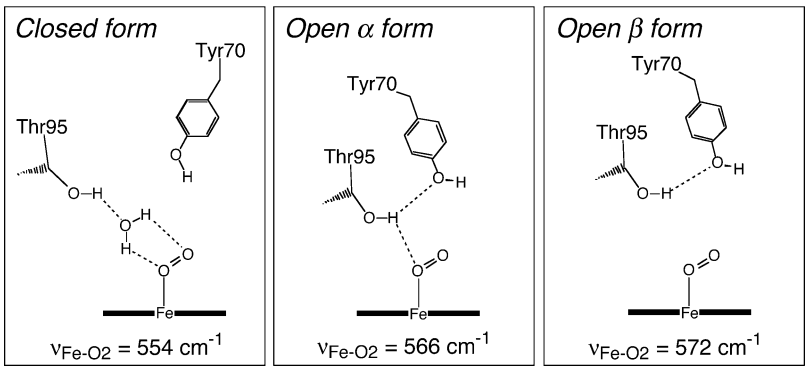

4C (a)], which are almost the same positions as those of WT, indicating that the Y70F mutant has the same closed and open forms as WT. These results suggest that H-bonding between Tyr70 and heme-bound O_2 does not exist even in the closed form, and rather that the orientation of the phenyl ring at position 70 (benzene ring for the Y70F mutant) relative to the heme-bound O_2 would be responsible for distinguishing the closed form from the open forms. Although Tyr70 is oriented toward the heme-bound O_2 in the closed form (Figure 3B right), the side chain of Tyr70 would be flipped out of the heme pocket in the open forms of O_2-bound HemAT-*Bs*, as observed in the unliganded structure of the sensor domain (Figure 3B left).[84] The Y70F mutant gave the same three ν_{Fe-O_2} bands as did WT, but the population ratios of the open to closed forms were altered between the WT and Y70F mutants, as can be seen in Figure 4A (a) and 4C (a). The ratio of the closed to open forms increased in the Y70F mutant compared to WT, and the reason for this result remains to be clarified.

A schematic diagram of the multiple conformations of O_2-bound HemAT-*Bs* is presented in Scheme 1. Whereas CO-bound hemoproteins are known to form multiple conforma-

tions [open (A_0) and closed ($A_1 + A_3$) forms],[85] this is the first example of an O_2-bound hemoprotein that demonstrates the presence of multiple conformations from the ν_{Fe-O_2} RR bands. Although Yu et al. previously observed multiple ν_{O-O} bands in O_2-bound cobalt-substituted hemoglobin and ascribed it to the presence of the multiple conformations of the Co−O_2 moiety,[72] later, the idea of the multiple conformations was interpreted differently by Bruha and Kincaid.[75] Thr95 would be crucial for the specific sensing of heme-bound O_2, whereas Tyr70 would be essential for the signal transduction from the heme pocket to the signaling domain.[84] In one of the open forms that has weak hydrogen bonding, a H-bond donor to the bound O_2 would be a protein residue, because the ν_{Fe-O_2} band around 566 cm^{-1} demonstrated clearly a H_2O/D_2O frequency shift. Because the H-bonding protein residue would not be displaced in D_2O compared to that in H_2O, the distance of the D-bond to O_2 would be greater than the distance of the H-bond to O_2 because of difference in the zero-point energies in the asymmetric vibrational potential by anharmonicity, which would result in a weaker D-bond strength,[86] as indicated by the upshift of the ν_{Fe-O_2} band. Such a feature was first noticed for Co-substituted oxyMb and oxyHb,[73] and it is now observed for various oxy heme proteins. Presumably, Thr95 is the H-bonding protein residue. Because X-ray analyses of CN-ligated HemAT-*Bs* have shown that the carbonyl group of Leu92 is involved in a H-bonding network around the bound ligand through an interaction with the water molecule,[84] Leu92 might be important for the synchronous movement of Thr95 and Tyr70 for the formation of the multiple conformations of O_2-bound HemAT-*Bs*.

The RR spectrum of the truncated sensor domain is shown in Figure 4B (a), where the oxygen-isotope-sensitive bands of protein were fitted with two Gaussian bands centered at 563 and 571 cm^{-1}. Therefore, truncation of the linker and signaling domains affected only the closed form, which disappeared in this truncated protein, although the open forms with ν_{Fe-O_2} at 566 and 572 cm^{-1} are little influenced. In other words, the closed form has a structural linkage with the signaling domain.

Although the ν_{O-O} RR band of WT HemAT-*Bs* was difficult to identify because of the congested region of the spectrum, we could determine the ν_{O-O} frequency for the truncated sensor domain at 1126 cm^{-1}, as shown in Figure 5. The RR enhancement of the ν_{O-O} band was extremely weak and overlapped with some heme vibrational modes, but we could identify the ν_{O-O} bands in the $^{16}O_2 - {}^{18}O_2$ difference spectrum (c) as indicated by the set of positive and negative peaks at 1126 and 1063 cm^{-1}, respectively. Presumably, the other ν_{O-O} band is too weak to be observed. The ν_{O-O} frequency at 1126 cm^{-1} is consistent with a ferric iron superoxide configuration ($Fe^{3+}-O-O^-$) but not with a ferrous iron neutral oxygen complex ($Fe^{2+}-O=O$).[87,88] Thus, the O_2 ligand is significantly polarized.

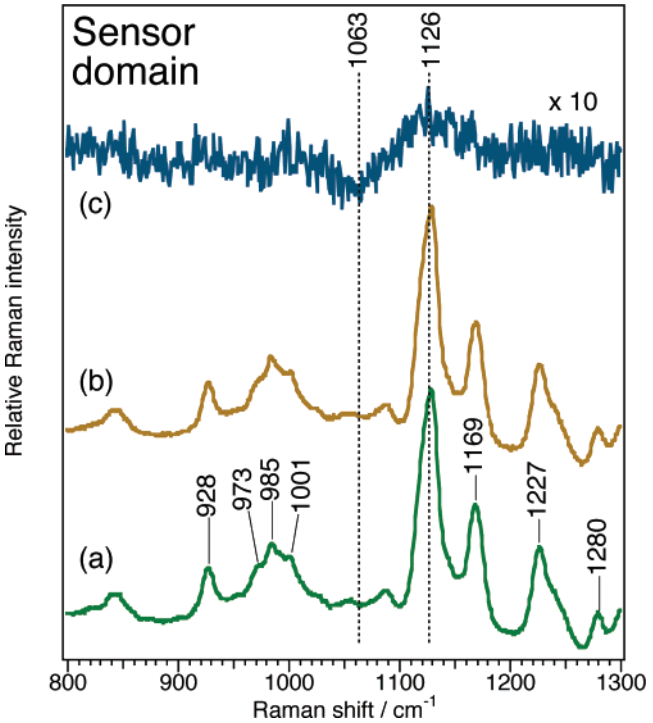

Figure 5. RR spectra in the ν_{O-O} region of the O_2-bound truncated sensor domain protein of HemAT-*Bs*: (a) $^{16}O_2$- and (b) $^{18}O_2$-bound forms and (c) $^{16}O_2$-minus-$^{18}O_2$ difference spectrum.

To date, only a few examples of the simultaneous observation of ν_{Fe-O_2} and ν_{O-O} have been reported for histidine-coordinated hemoproteins.[78] The charge transfer (CT) from heme to the bound oxygen upon Soret excitation, which could be increased by the strong H-bonds from the distal environment to the bound O_2, would be an important factor for the simultaneous appearance of the ν_{Fe-O_2} and ν_{O-O} bands in the RR spectra. The ν_{Fe-O_2} frequencies are plotted against the ν_{O-O} frequencies in Figure 6 for the available data. It is possible to describe these data as falling on a straight line, except for imidazole-coordinated model compounds, as expected from the d_{z^2}-controlled d_π back-donation mechanism that determines these frequencies.[56] Alternatively, there could be two direct correlation lines, one for 6c imidazole-coordinated model compounds and one for 6c thiolate complexes, or the effects on the correlation could be sufficiently multidimensional that the true correlation(s) are not apparent from Figure 6.

Whereas heme-bound O_2 interacted strongly with the distal side, the properties of the ν_{Fe-CO} and δ_{Fe-C-O} RR bands indicated that heme-bound CO does not interact with the distal side.[32] Indeed, the RR spectral features of the CO-bound form of the truncated sensor domain, T95A, and the Y70F mutants are almost the same as those of WT.[34] Thus, CO is discriminated by HemAT-*Bs*. In the case of NO, the ratios of the 6c and 5c heme−NO adducts are altered between WT and the truncated sensor domain protein.[34] Thus,

(85) Morikis, D.; Champion, P. M.; Springer, B. A.; Sligar, S. G. *Biochemistry* **1989**, *28*, 4791−4800.
(86) For detail on the relative energies of hydrogen and deuterium bonds due to differences in zero-point vibrational energy discussed in terms of a quantum chemical calculation at the SCF and correlated MP2 levels, see: Scheiner, S.; Cuma, M. *J. Am. Chem. Soc.* **1996**, *118*, 1511−1521.
(87) Weiss, J. J. *Nature* **1964**, *202*, 83−84.
(88) Momenteau, M.; Reed. C. A. *Chem. Rev.* **1994**, *94*, 659−698.

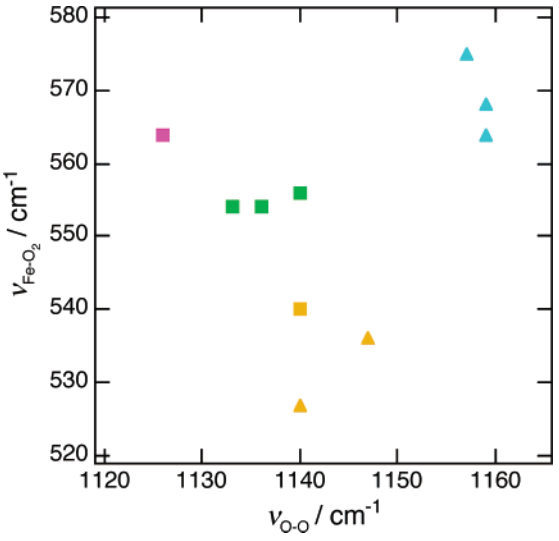

Figure 6. Correlation between frequencies of ν_{Fe-O_2} and ν_{O-O}. Truncated sensor domain determined by the positive peaks of the difference spectra (pink square), *Synechocystis* and *Chlamydomonas* Hb's (green squares), cytochrome P450 (orange square), imidazole ligated 6c model heme (blue triangles), cysteinate ligated 6c model heme (orange triangles). The reference data were taken from ref 78.

a proximal signaling pathway triggered by strain on the Fe−His bond might be important for discrimination against NO.

As a summary of this section, O_2 is specifically sensed by the distal environment of HemAT-*Bs*, which has a long-distance structural linkage with the signaling domain. Importantly, our RR studies revealed the presence of a H-bond network in the distal environment for sensing O_2. The multiconformational property of the distal side should play a central role in regulating the enzymatic activity as well as sensitivity to O_2, and it is desirable to understand what factors control the distal rearrangement in terms of O_2 concentration and interaction with signaling proteins engaged in the signal transduction cascade.

Sensing Mechanisms of Other O_2 Gas Sensory Proteins

Next, we discuss the proposed sensing mechanisms of other O_2 gas sensory proteins. The examples included here were investigated extensively by RR spectroscopy and/or X-ray crystallography.

FixL. The CO affinity of FixL is 100 times lower than that of Mb, but the binding affinity for O_2 is not as high as that expected for an O_2 sensor. Thus, the discrimination against CO by FixL should not be based on its ligand binding affinities, but should include other mechanisms such as ligand-dependent allostery.[3] *Bj*FixLH, a sensor domain from *Bradyrhizobium japonicum* FixL, was initially investigated by X-ray structural analyses, and currently, the crystal structures of the ferric and ferrous forms and CO-, NO-, O_2-, CN-, imidazole-, and methyl imidazole-bound forms are available, as shown in Figure 7.[12,16,19] On the basis of the crystal structural information, it was proposed that binding of strong-field ligands to the heme initiates the conformational change by inducing a flattening of the heme plane. This helps to reduce the strength of the interaction between the critical arginine (Arg220) and heme-propionate 7 and provides a mechanism for discriminating the binding of strong-field ligands, such as O_2, from that of weak-field ligands. This Arg220 can then be used to discriminate O_2 from CO and NO by differentiating the affinity of this ligand to H-bond to the arginine side chain. Rotation of Arg220 into the heme pocket that occurs upon binding of O_2 serves as steric hindrance against Ile215, resulting in conformational changes in the distal side called the FG loop and thus in stabilization of the kinase inactive form. If Arg220 cannot form a H-bond to a heme-bound ligand as for CO and NO, the resulting conformational change is small in the FG loop. Thus, it was proposed that Arg220 plays a crucial role in FixL ligand discrimination and allostery.[12,16,19]

For the sensor domain of FixL from *Rhizobium meliloti* (*Rm*FixLH), crystal structures are limited to the unligated form,[17] but extensive RR and other spectroscopic studies were performed.[10,11,13−15,17,18] Actually, distal influences on ligand discrimination by *Rm*FixL were first suggested by RR data.[10] In an RR study,[17,18] the ν_{Fe-O_2} frequency was determined to be 575 cm^{-1} for *Rm*FixLH, but the frequency exhibited a 5 cm^{-1} downshift upon replacement of distal isoleucine (Ile209) with alanine (the residue lining the distal environment of *Rm*FixL is different from that of *Bj*FixL). On the basis of the RR observation, it was proposed that, because of a steric effect of bulky Ile209, Fe−O−O is more distorted in the *Rm*FixLH WT form than in the I209A mutant. An EXAFS study of O_2-bound *Rm*FixLs with and without the kinase domain demonstrated that the Fe−O−O angles were different between the two forms, indicating that the distal side of the heme-based sensory domain that interacts with the heme-bound O_2 has a structural linkage with the kinase domain.[13] Thus, distal steric interactions have been emphasized in the O_2 sensing mechanism of *Rm*FixL,[17,18] whereas the deformation of heme triggered by binding of a strong-field ligand was proposed as the initial event of the sensing mechanism of *Bj*FixL.[12,16,19]

Rodgers et al. carried out a dynamic RR study on the photodissociation of CO-bound *Rm*FixLH using a nanosecond pulsed laser.[14] The nanosecond dynamics provided the first glimpse of how FixL begins its transformation from an inactive 6c low-spin species to an active 5c high-spin species, as illustrated by Scheme 2, although CO is not an actual inhibitor of FixL. In this RR dynamics study, transient strengthening of the proximal Fe−His bond relative to the equilibrium deoxy form was revealed by an increased Fe−His stretching frequency. Thus, Rodgers et al. proposed that FixL's ability to generate transient strain in its Fe−His bond provides one means of propagating conformational motion to its kinase domain in response to changes in O_2 tension.

***Ec*DOS.** The heme-based sensor domain of *Escherichia coli* DOS (*Ec*DOSH)[22−25] is also a heme-PAS domain, but some properties of *Ec*DOSH differ from those of FixLH. For example, ferrous *Ec*DOSH contains a 6c low-spin heme, and when an exogenous ligand nears, the original sixth ligand from the protein is replaced by the exogenous ligand. Evidence for this was obtained by site-directed mutagenesis

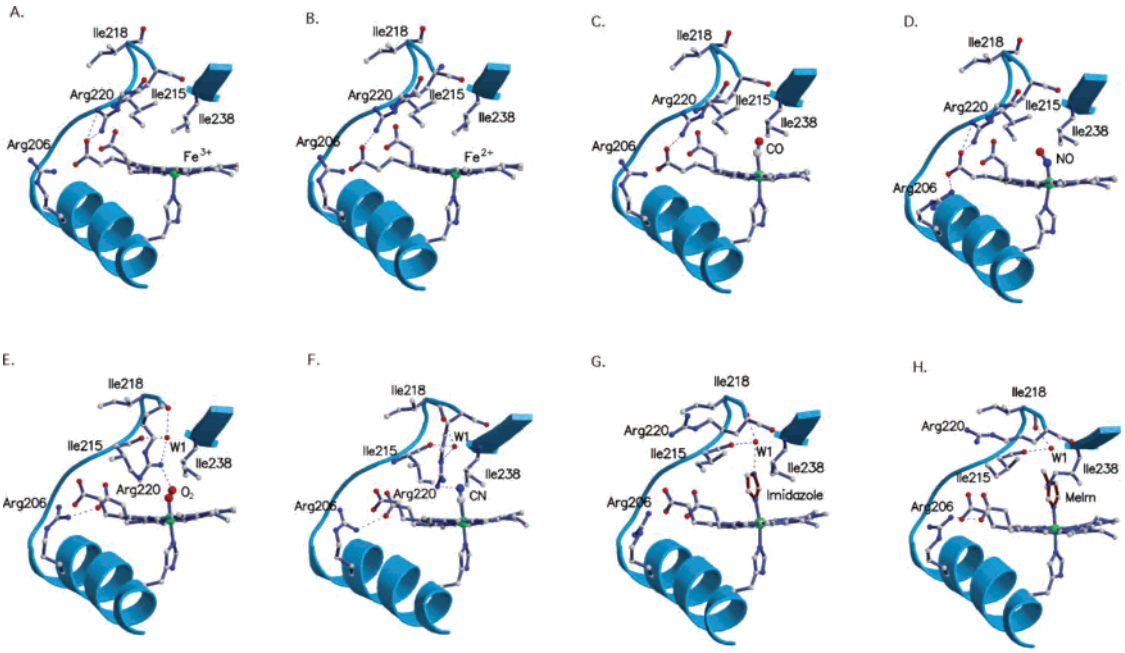

Figure 7. Ribbon and ball-and-stick model diagrams of the *Bj*FixLH heme-binding pockets for (A) met-*Bj*FixLH, (B) deoxy-*Bj*FixLH, (C) CO-*Bj*FixLH, (D) NO-*Bj*FixLH, (E) O_2-*Bj*FixLH, (F) cyanomet-*Bj*FixLH, (G) imidazole-*Bj*FixLH, and (H) MeIm-*Bj*FixLH. Reprinted with permission from ref 19. Copyright 2002 American Chemical Society.

Scheme 2

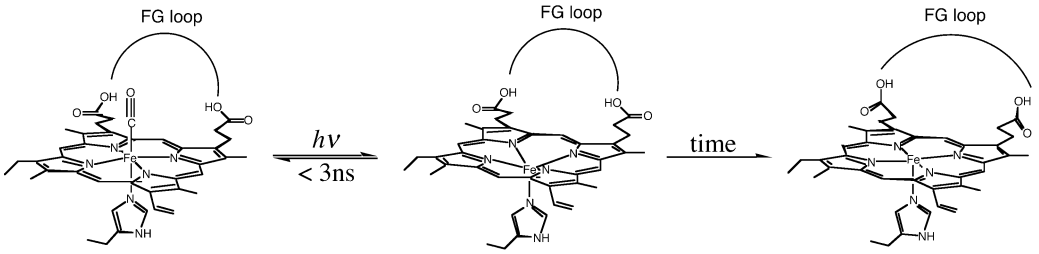

experiments in combination with RR spectroscopy that implicated His77 and Met95 as heme ligands in *Ec*DOSH.[23,24] In the RR spectrum of O_2-bound *Ec*DOSH, the ν_{Fe-O_2} band was located at 561 cm^{-1}, which is considerably lower than that of Mb.[23,24] Thus, the existence of hydrogen bonding between the proximal oxygen atom and distal amino acid residue(s) was suggested to be responsible for the low frequency of O_2-bound *Ec*DOSH. The strong H-bonding would stabilize the bound O_2, and this is consistent with the low O_2 dissociation rates observed for O_2-bound *Ec*DOSH ($k_{off} = 0.032\ s^{-1}$). On the other hand, the RR spectrum of CO-bound *Ec*DOSH was indicative of the linear and upright Fe−C−O structure consistent with a hydrophobic distal environment.[23,24] Thus, the heme-bound CO is discriminated, whereas the proximal O atom of iron-bound O_2 forms a strong H-bond with distal residues. Recently, X-ray structures have been determined for the truncated sensor domain protein (*Ec*DOSH).[25] The *Ec*DOSH protein was crystallized in a dimer form, and heme in only one subunit bound O_2. In the O_2-bound monomer, the Arg97 side chain reorients inward to the heme distal pocket to provide stabilization to heme-bound O_2. The role of Arg97 is that of a hydrogen-bond donor, displaying Arg−N···O (heme-bound proximal oxygen) distances of 2.70 and 2.94 Å, indicating that, as expected from RR spectroscopy, the proximal O atom of heme-bound O_2 is incorporated into the H-bonding network from the distal environment. Thus, the distal sensing mechanism would be predominant in *Ec*DOSH, as shown schematically in Figure 8.

***Tt*Tar4H**. The heme domain of *T. tengcongensis* Tar4 protein, *Tt*Tar4H, is reported to be sGC-like and to bind both NO and O_2 and thus is referred to as a H−NOX domain characterized by a "YxTxR" motif.[43−45] However, a heme of sGC does not bind O_2, probably because of a large negative field of the heme pocket that could readily increase the O_2 dissociation rate, precluding binding.[55] The ν_{Fe-O_2} frequency detected by RR spectroscopy for O_2-bound *Tt*Tar4H is 567 cm^{-1},[44] indicating that the distal interaction to the heme-bound O_2 is moderate. Another sGC-like heme domain from *Vibrio cholerae* (VCA0720) is unable to bind O_2, but interestingly, it binds NO, forming a 5c NO adduct as in the case of sGC.[44] The two homologues of the sGC heme domains exhibit significantly different coordination chemistries with NO, CO and O_2, and the reported characters,

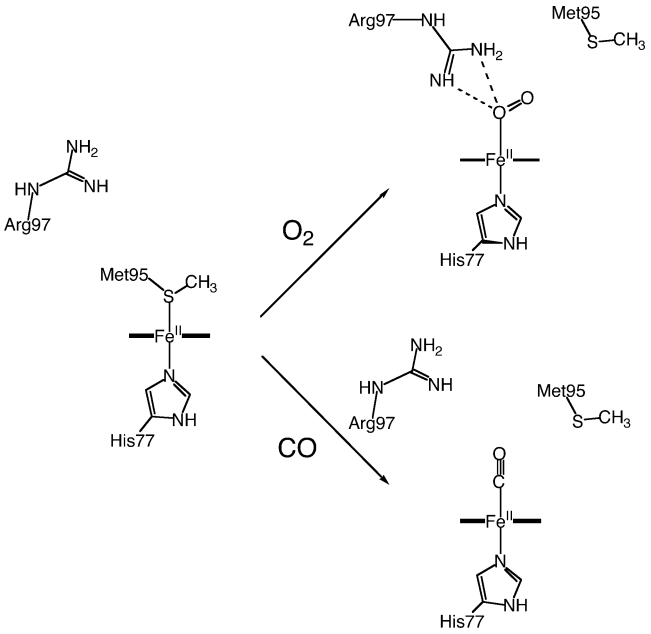

Figure 8. Possible O_2 and CO discrimination mechanism of *Ec*DOSH.

Table 2. Fe−Ligand and Ligand Internal Vibrations (cm^{-1})[a]

	ν_{Fe-His}	ν_{Fe-CO}	ν_{C-O}	ν_{Fe-NO}	ν_{N-O}	ν_{Fe-O_2}
sGC	204	472	1987	525	1677	
VCA0720	224	491	1985	523	1674	
*Tt*Tar4H	218	490	1989	553	1655	567
Mb	220	512	1944	554	1624	570

[a] Reference data were taken from ref 44.

which are based to a significant extent on RR data, are summarized in Table 2.

Recently, the X-ray structure of the O_2-bound H−NOX domain was reported by Kuriyan and co-workers.[45] Residues lining the distal pocket are exclusively nonpolar, with the exception of Tyr140, the side chain of which forms a H-bond with the O_2 ligand, as shown in Figure 9. The orientation of Tyr140 is fixed by a H-bonding network involving Trp9 and Asn74, which might contribute to the high affinity of the protein for O_2.[45] The most remarkable feature of the O_2-bound H−NOX domain is the highly nonplanar porphyrin group. Although the deviation from planarity is common in protein-bound heme groups, the extent of the distortion observed for the H−NOX domain is unprecedented among hemoproteins for which crystal structures are available.[45] Thus, the heme distortion was proposed to be an important signaling mechanism of the H−NOX domain.[45] RR spectroscopy is a sensitive tool as a probe of heme distortion.[89−91] Desbois et al., on the basis of an RR study for a series of strapped model heme compounds, related the increased heme distortion with a decrease in O_2 ligand off rates.[90] The decrease was specific for O_2 (but not CO) off rates in the models. Thus, the heme distortion in the H−NOX domain

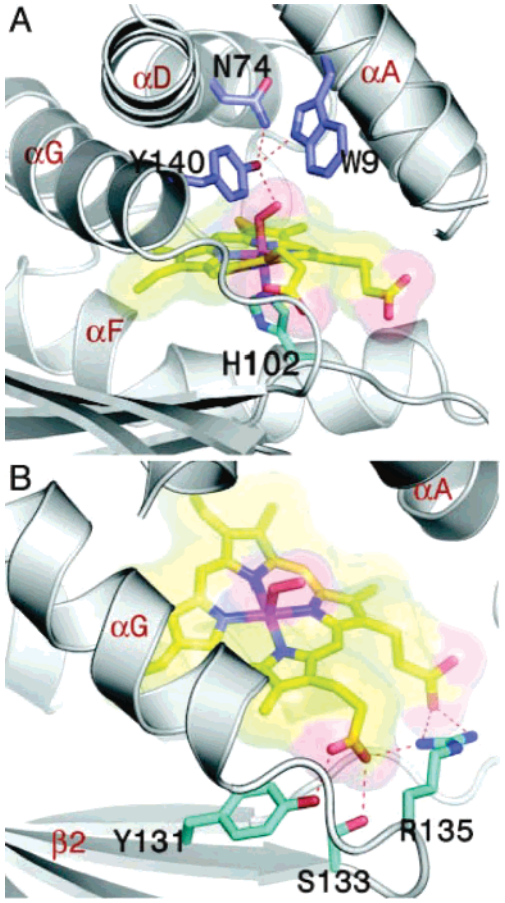

Figure 9. Heme environment of the O_2-bound H−NOX domain. (A) Ligand-binding pocket. (B) YxSxR motif, corresponding to residues Tyr131, Ser133, and Arg135, that coordinates heme propionates. Reprinted with permission from ref 45. Copyright 2004 National Academy of Sciences.

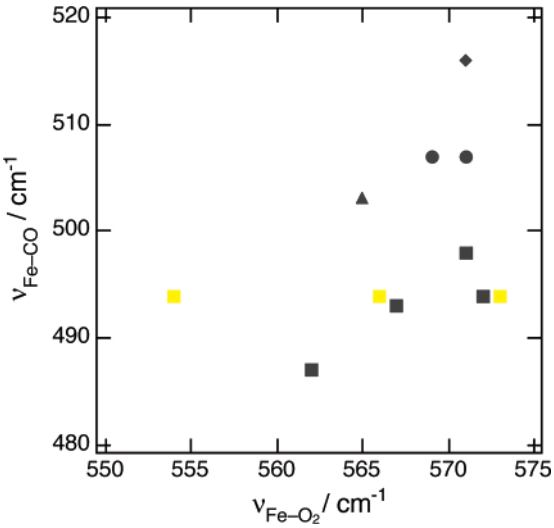

Figure 10. Correlation between the frequencies of ν_{Fe-O_2} and ν_{Fe-CO}. HemAT-*Bs* (yellow squares), O_2 sensor hemoproteins (black squares), heme oxygenase (black triangle), Hb and Mb (black circles), bovine cytchrome c oxidase (black diamond). There are three markers for HemAT-*Bs* because of the multiple ν_{Fe-O_2} bands. The data were taken from refs 20, 32, 59, and 79.

can provide a mechanism for discrimination between CO and O_2 binding.

As a summary, each O_2 sensor protein has a unique way to discriminate ligands at the heme sensing unit. Despite this

(89) Prendergast, K.; Spiro, T. G. *J. Am. Chem. Soc.* **1992**, *114*, 3793−3801.
(90) Desbois, A.; Momenteau, M.; Lutz, M. *Inorg. Chem.* **1989**, *28*, 825−834.
(91) Picaud, T.; Moigne, C. L.; Loock, B.; Momenteau, M.; Desbois, A. *J. Am. Chem. Soc.* **2003**, *125*, 11616−11625.

variation, O_2 sensor proteins generally achieve greater sensitivity by utilizing the allosteric effect specific to the target molecule. In the case of the O_2 carrier Mb, however, a ligand-dependent conformational change in the distal side is not significant, as can be seen from the X-ray crystal structures of CO, NO, and O_2-bound Mb.[92] Therefore, for example, plots for the ν_{Fe-O_2}/ν_{Fe-CO} correlation make a sort of groups depending on the functions of hemoproteins that utilize O_2, as shown in Figure 10. It seems likely that there is a general and direct correlation between protein environmental effects on the Fe−O_2 and Fe−CO stretching frequencies. This correlation plot suggests that the distal sides of heme-bound CO in O_2 sensor hemoproteins are hydrophobic, yielding relatively low Fe−CO stretching frequencies in contrast with slightly wider distribution of the ν_{Fe-O_2} frequencies, and in some cases, heme-bound O_2 interacts strongly with the distal environment, showing relatively low ν_{Fe-O_2} frequencies.[93] Hence, the ligand-dependent allostery is a key mechanism of O_2 gas sensory hemoproteins.

(92) Olson, J. S.; Phillips, G. N. *J. Biol. Inorg. Chem.* **1997**, *2*, 544−552.

(93) Regarding the wide distribution of the ν_{Fe-O_2} frequencies of WT HemAT-*Bs*, a reviewer pointed out that the existence of the 554 cm^{-1} component is not firmly established because of the small isotope shifts (17−18 cm^{-1}) and very similar $^{16}O_2 - {}^{18}O_2$ difference spectra for all samples, as shown in Figure 4. Still, we believe that the 554 cm^{-1} component is present in WT HemAT-*Bs*, because the sensor domain protein does not have such a strongly H-bonded form, and therefore, its raw RR spectrum in the ν_{Fe-O_2} region is significantly different from that of WT.

Conclusion

RR spectroscopy is a highly sensitive tool for studying heme-bound diatomic molecules. Our studies on the O_2 sensor HemAT-*Bs* protein reveal that heme-bound O_2 is sensed by the distal side among multiple conformation mixtures. The structural linkage between the distal heme environment and effector domain that we found in the study of WT and truncated sensor domain protein is the peculiar nature of the heme-based gas sensory proteins. The next important issues in the study of the gas sensory proteins are to elucidate the mechanisms of the allosteric pathway and the dynamics of the protein that might be responsible for the regulation of the enzymatic activity as well as the sensitivity to O_2.

Acknowledgment. We are grateful to Prof. Shigetoshi Aono, Dr. Shiro Yoshioka, and Mr. Hideaki Yoshimura for providing us the HemAT-*Bs* proteins for RR measurements. This study was supported by the JSPS Research Fellowship for Young Scientists to T.O. and by a Grant-in-Aid for Specifically Promoted Research to T.K. (14001004).

IC0486318